A R C H I V E S O F M E T A L L U R G Y A N D M A T E R I A L S
Volume 58 2013 Issue 4
DOI: 10.2478/amm-2013-0130

A. ŚWIĄTONIOWSKI*, O. BAR**

MATHEMATICAL MODELLING OF THE HIGH FREQUENCY VIBRATIONS DURING COLD ROLLING PROCESS

MATEMATYCZNE MODELOWANIE DRGAŃ WYSOKOCZĘSTOTLIWOŚCIOWYCH WYSTĘPUJĄCYCH PODCZAS WALCOWANIA BLACH NA ZIMNO

The study explores the model of high-frequency vibrations during the continuous rolling processes, the underlying assumption being that vibrations are self-excited. The effects of rolling stand and rolling process parameters on the nature and intensity of vibrations are investigated. The appearance of darkened streaks occurring on the metal sheet is explained. The results are compared with the data quoted in literature on the subject.

Keywords: rolling stand, self-excited vibrations, high-frequency vibrations, Timoshenko beam model

W pracy przedstawiono model opisujący drgania o wysokiej częstości, występujące w trakcie ciągłego walcowania blach. Model ten jest oparty na założeniu samowzbudności procesu. Zbadano wpływ parametrów klatki oraz procesu walcowania na charakter i intensywność drgań. Wyjaśniono również zjawisko powstawania na powierzchni blachy zaciemnionych pasków. Otrzymane wyniki porównano z wynikami badań.

1. High-frequency vibrations

Modern machines and means of transport are required to be more and more energy- efficient and ready to deliver a long and failure-free performance. Fulfilling of these requirements would be impossible but for the materials engineering which allows to develop and introduce new building materials of extremely high structural strength and hardness which are nevertheless resistant to plastic working. Such conditioning together with application of higher and higher deformation speed (up to 100 s^{-1}) contribute to the appearance of vibrations in the course of plate and band rolling.

These vibrations are in certain circumstances excited by relatively small and nearly invisible parameters disturbances. They manifest long exposure time and fall into two intervals depending on vibration frequency mainly 125-256 HZ and 700-1000 HZ [6, 7, 9, 14- 22].

The first interval embraces vibrations leading to fluctuation in band thickness, sometimes even its rupture. They have been broadly discussed in various papers, to name just a few: [9-12].

Such threat does not appear in case of high-frequency vibrations which do not have substantial influence on the thickness of a rolled band. However, they may bring about the appearance of visible, lateral, alternately bright and dark strips on the surface of rolled metal plates with a constant λ scale amounting to about 30 [mm] specific for a certain type of rolling mills and process parameters. Roughness created this way may fluctuate between 3-30 μm [13-20]. Metal plates of this sort are perceived to be products of poor quality mainly due to the fact that the a.m. strips may show through the anti-corrosion and ornamental coatings. As a result, they cannot find application in car bodies, casing of household appliances or metal packaging.

Generally, the basic vibration mechanism of the four-high temper rolling mills in the frequency range 500-1000Hz (fifth octave mode chatter) – that lead to marks on the steel strip surface – is believed to be parametrical and self-excited [1, 9, 10, 12, 23].Closer analysis of the problem, however, allows to notice that some of the assumptions made in studies carried out to date, particularly the ones concerning occurence and values of the phase shift between rolling force and vertical vibration of the rolls in a stand [6, 11], do not find their ultimate support in the presented mathematical descriptions.

Despite numerous attempts, the essence of these phenomena has not been faithfully described yet which may have its source in great difficulties in analyzing self-excited vibrations found in mass-spring systems e.g. in a rolling mill.

Furthermore, there has been not enough data gathered in order to define the conditions in which such a vibration occurs and subsequently to reduce it thanks to introducing new construction solutions as well as adjusting the process parameters.

In order to overcome the a.m. difficulties it has been assumed in this paper that the vibration of four-high mill's rolls may be described in a form of the Timoshenko beam [19,24].

* AGH UNIVERSITY OF SCIENCE AND TECHNOLOGY, FACULTY OF MECHANICAL ENGINEERING AND ROBOTICS, AL. A. MICKIEWICZA 30, 30-059 KRAKÓW, POLAND
** PEDAGOGICAL UNIVERSITY OF CRACOW, 2 PODCHORĄŻYCH STR., 30-084 KRAKÓW, POLAND

The action of the strip on the work rolls, which results from its plastic deformation, has been described using Sims formula.

The numerical simulation of the system have been done using real parameters value of the industrial four-high rolling mill.

It has been shown that criterion of the investigated vibration occurence must be considered including the form of transverse vibration of the strip coupling the neighboring stands of the series.

2. Underlying assumptions

It is assumed that the relative motion of centers of section of the working and backing rolls is negligible and hence can be omitted due to Hertz contact stress formulae. Hence they can be replaced by a one short, equivalent roll, based on the Timoshenko model. Its parameters are adjusted such that the first three natural frequencies of the real and equivalent objects should coincide.

•In accordance with the widely adopted methodology, the rolling stand is modeled by a motionless mass-free elastic element, with no damping. Its rigidity is assumed as in [3].

•The band is assumed to be a non-inertial element [5].

•According to Huber's hypothesis axial stress pulsation in the band, associated with changes of its thickness, will change the value of the reduced yield point. This parameter directly affects the force of streak-roll interaction. There is a phase shift between this force and variable axial stresses in the band, well documented in [4,5]. Under medium-frequency vibrations, it attains large values, amounting even to $\pi/2$ in the case of the stability loss. In the case of high frequency vibrations, we assume that it is small. The phase shift value is evaluated on the basis of numerical simulation data.

•The vertical impact acting upon equivalent rolls is governed by the Sims formula. Instead of modifying the reduced stress, the phase shift is introduced into the function w(x,t), describing the vertical motion of the section.

$$q_1 = \sigma^* \sqrt{R[\Delta h_0 + 2w(x, t - \tau_0)])} \tag{1}$$

The following designations are used: σ^*-yield stress, Δh_0 – steady-state draft, τ_0 – phase shift, w- coordinate expressing the vertical motion of the roll section with the coordinate x.

•The description of damping assumes that energy dissipation takes place only in the plasticized band section in the rollgap. Stress measured in the direction vertical to the plane of the metal sheet being rolled is governed by the formula $\sigma = \varepsilon_1 \dot{y} + \varepsilon_2 \dot{y}^3$ The variable y expresses the variations of the band section height depending on its position in the rollgap.

3. Parameters of the equivalent roll

Fig (1) shows the model of the upper section of the four high rolling stand, further utilised in numerical analysis. It comprises an equivalent roll with the constant diameter R, pressed to the band by springs with stiffness c_0. These springs model the stand housings with the pressing elements. Parameters: R, c_0 and equivalent density ρ of the material have to be precisely controlled to ensure that the first three natural frequencies of the model should coincide with the relevant frequencies of the real system. The upper and lower parts of the rolling stand, separated by the band, are assumed to be symmetrical.

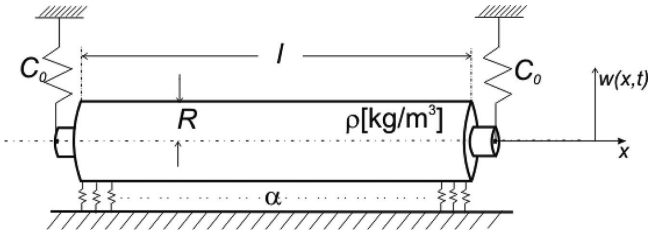

Fig. 1. Rolling stand model: R-equivalent radius, ρ – equivalent density, c_0 – stand rigidity in the vertical direction

Distributed (reduced to two dimension) action of the immobile band upon the equivalent roll can be approximated by a linear relationship, with a sufficient accuracy. Recalling (1):

$$q_{10} = \sigma^* \sqrt{R\Delta h} = \sigma^* \sqrt{R[\Delta h_0 + 2w(x,t)]} \cong \sigma^* \sqrt{R\Delta h_0} \left[1 + \frac{w(x,t)}{\Delta h_0}\right] =$$
$$= q_{00} + q_1 = q_{00} + \alpha w(x,t) \;;\; \alpha = \sigma^* \sqrt{\frac{R}{\Delta h_0}} \tag{2}$$

The expression $\Delta h_0 = h_{10} - h_{20}$ stands for the draft during the steady rolling process. In this approach the dynamic model shown in Fig (1) can be brought down to that of the Timoshenko's beam supported on the linear, elastic base. Partial equations and the associated boundary conditions are written as [24,25]:

$$w_{xx} - \frac{k\rho}{G} w_{tt} - \frac{\alpha k}{GA} q_1(x,t) = \vartheta_x$$
$$\vartheta_{xx} - \frac{\rho}{E} \vartheta_{tt} = -\frac{GA}{kEJ}(w_x - \vartheta) \tag{3}$$

with boundary conditions:

$$M(0,t) = -EJ\vartheta_x(0,t) = M(l,t) = -EJ\vartheta_x(l,t)$$
$$T(0,t) = \tfrac{GA}{k}\,[w_x(0,t) - \vartheta(0,t)] = c_0 w(0,t)$$
$$T(l,t) = \tfrac{GA}{k}\,[w_x(l,t) - \vartheta(l,t)] = -c_0 w(0,t)$$

where: $w_x = \frac{\partial w}{\partial x}, w_t = \frac{\partial w}{\partial t}, w_{xx} = \frac{\partial^2 w}{\partial x^2}, w_{tt} = \frac{\partial^2 w}{\partial t^2}, \vartheta$ -angle of rotation section, E and G denote the Young modulus and Kirchoff modulus, respectively and $k-$geometric warping factor, equal to 10/9 for circular cross-sections; A, J – surface area and the moment of inertia of the roll cross-section.

$$q_1(x,t) = \alpha w(x,t) \tag{4}$$

Substituting (4) into (3) yields a linear system of differential equations governing the rolling stand behaviour whilst the band remains immobile. Thus, one is able to obtain and further optimise the natural frequencies to make sure they agree well with the data of real construction.

The second frequency $f_2 \cong 150[Hz]$ is associated with medium-frequency vibrations, $f_4 \cong 730[Hz]$ – with high-frequency vibrations. The results were obtained for the following parameters of the rolling mill:

R =0.4[m] – roll radius,

ρ =36423[kg/m^3] – equivalent density of the rolled material,

c_0 =0.895*10^{10}[N/m] – equivalent stiffness of the rolling stand with the rolled material

l =1.2[m] – roll length

σ^* =3*10^8[N/m^2] – yield stress,

Δh_0 =0.2*10^{-3}[m] – draft,

$\alpha = 0.671 * 10^{10}$[N/m^2]

Accordingly, we get:

TABLE 1

Natural frequencies of the system

i	ω_i[rad/s]	f_i[Hz]
2	1047.14	160.7
3	1432.06	228
4	4559	726

It is readily apparent that the quantity ρ has a non-physical nature. It has no bearing, however, on further calculations. Natural modes was identified as progressive (the second) and symmetrical (the fourth). The third form, antisimetrical in this case is negligible.

Fig(2) shows the natural modes coupled with natural frequencies f_2 and f_4.

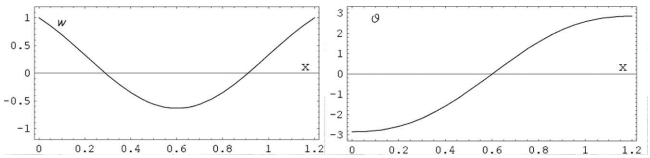

Fig. 2. Fourth (symmetrical) natural modes associated with high-frequency vibrations

4. Dynamic action of a band upon the equivalent roll

This interaction is expressed as the sum of two components: that involving band plasticisation and progressive motion and that associated with the viscous friction force.

4.1. Impact of the plasticised band section

In accordance with the assumption yielding the relationship (1), dynamic overloading involved in the band interaction force and taking into account its lifting motion is expressed as:

$$q_1^d(x,t) = \alpha w(x, t-\tau_0) \quad ; \quad \alpha = \sigma^* \sqrt{\frac{R}{\Delta h_0}} \tag{5}$$

This form of distributed loading renders the equations of motions extremely difficult to solve numerically. That is why the function $w(x, t-\tau_0)$ shall be replaced by its approximation based on the assumption that it deviates only slightly from the harmonic function $w_t = \omega_4 X(x)\cos(\omega_4 t)$

$$w(x,t-\tau_0) = X(x)\sin(\omega_4 t)\cos(\omega_4\tau_0) - X(x)\cos(\omega_4 t)\sin(\omega_4\tau_0) = \cos(\beta)w(x,t) - \frac{\sin(\beta)}{\omega_4} w_t(x,t)$$

Hence the delayed argument function is replaced by a linear combination of functions w and w_t and the second term can be thus interpreted as negative damping.

4.2. Band-roll interaction due to energy dispersion

Interactions associated with damping are referred to as q_2. Under the assumption made, the stress on the roll-band interface is governed by the formula:

$$\sigma_T = \varepsilon_1 \dot{y} + \varepsilon_2 \dot{y}^3 \tag{6}$$

Parameters ε_1 and ε_2 are associated with damping and will be obtained by numerical simulations. The interpretation of the variable y is shown in Fig (3).

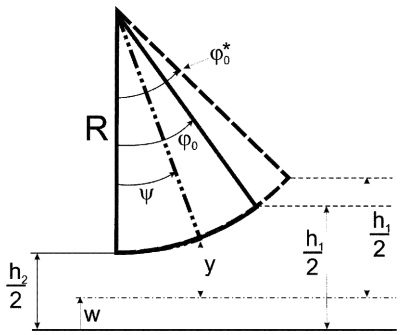

Fig. 3. Geometry of the roll bite- schematic diagram

Here the motion of the roll's centre is replaced by the motion of the band's axis. Axis position remains unchanged despite the vibrations, due to the backward motion of the working rolls. Fig (3) leads to simple relationships:

$$\frac{h_2}{2} + R = R\cos\phi_0 + \frac{h_1}{2}; \frac{h_2}{2} - w + R = R\cos\phi_0^* + \frac{h_1}{2} \tag{7}$$

They relate the function w to the parameters ϕ_0 and ϕ_0^*

$$w = R(\cos\phi_0 - \cos\phi_0^*) \cong R\phi_0(\phi_0 - \phi_0^*)$$

Hence, after linearisation we get:

$$\phi_0^* = \sqrt{\frac{R}{\Delta h_0}} + \frac{1}{\sqrt{R\Delta h_0}} w$$

On the other hand, the relationship

$$\frac{h_2}{2} - w + R = R\cos\psi + y \tag{8}$$

is true which implies that when we assume the uniform rotary motion of the rolls with the velocity Ω, we get: $\dot{y} = -R\Omega\sin\psi - \dot{w}$ Combining these relationships yields the full loading q_2 due to damping, as given by the formula:

$$q_2 = -\int_0^{\phi_0^*} [\varepsilon_1 \dot{y} + \varepsilon_2 \dot{y}^3] R d\psi$$

Deleting the constant terms associated with the steady motion of the band (no vibrations), after necessary transformations we get the full dynamic loading of a roll due to the impacts of the band.

$$q_2^d = \alpha \left[\left(\frac{\varepsilon_1 \Delta h_0}{\sigma^*} + \frac{3}{8} \frac{\varepsilon_2 v^2 \Delta h_0^2}{\sigma^*} \right) \dot{w} + \frac{\varepsilon_2 \Delta h_0}{\sigma^*} \dot{w}^3 \right] \tag{9}$$

The introduced quantity $v = \Omega R$ is the speed at which the outer layers of the band leave the rollgap.

5. Differential equations of motion

Recalling the assumptions leads to the modification of equation (3), whereby the relevant functions are replaced. Quantities involving q_1^d and q_2^d, defined by (5), (6) and (10) describe partly linearised, dynamic interactions of the band in the elasticity and damping domain The transition from partial equations to an ordinary equation was performed using the Galerkin method. Thus modified equations (3) describe the self-excited process. In this case the applied Galerkin base is limited to one element, wherein base vector is selected as the eigenfunction corresponding to the frequency associated with the self-excited process. High-frequency vibrations correspond to the fourth mode, hence the vector is selected that corresponds to this particular frequency.

$$\mathbf{z} = \begin{bmatrix} w \\ \vartheta \end{bmatrix} = \begin{bmatrix} X_4(x) \\ \Phi_4(x) \end{bmatrix} u(t) \tag{10}$$

Its components X_4 and Φ_4 are shown in Fig (2) in column II.

Including (10) to PDE (3) and making standard calculations of the Galekin's method (ie. calculation inner product on the [0,l] range) we can reduce PDE to ODE equations.

The calculation procedure yields the equation describing and unknown function of time $u(t)$

$$\begin{aligned} &\left[\frac{k\rho c_1}{G} + \frac{\rho c_2}{E}\right]\ddot{u} + \frac{k\alpha\gamma_1 c_1}{GA}\dot{u} + \frac{k\alpha\gamma_2 c_3}{GA}\dot{u}^3 + \\ &+\left[\frac{k\alpha c_1}{GA} + \frac{GAc_2}{kEJ} + c4 - \frac{GAc_5}{kEJ} - c6 - c7\right]u = 0 \end{aligned} \tag{11}$$

Coefficients c_i are used to designate the following integrals:

$$\begin{aligned} &c_1 = \int_0^l X_4^2 dx \;;\; c_2 = \int_0^l \Phi_4^2 dx \;;\; c_3 = \int_0^l X_4^4 dx \;;\; c_4 = \int_0^l X_4\Phi_4' dx \\ &c_5 = \int_0^l X_4\Phi_4' dx \;;\; c_6 = \int_0^l X_4'' X_4 dx \;;\; c_7 = \int_0^l \Phi_4''\Phi_4 dx \;; \\ &\gamma_1 = \frac{-\sin(\beta)}{\omega_4} + \frac{\varepsilon_1\Delta h_0}{\sigma^*} + \frac{3}{8}\frac{\varepsilon_2 v^2 \Delta h_0^2}{\sigma^*}; \quad \gamma_2 = \frac{\varepsilon_2\Delta h_0}{\sigma^*} \end{aligned} \tag{12}$$

6. Results of the simulations

•Calculations were performed recalling Eq (11) and the following parameters:

σ^* =3.2*10^8[N/m2]	ρ =36423[kg/m^3]
ε_1 =1.8007*10^8[Ns/m^3]	c_0 =0.895*10^{10}[N/m]
ε_2 =3.2651*10^8[Ns^3/m^5]	$\Delta h_0 \in$(1.5,2.5)*10^4[m]
$\beta \in (\pi/10, \pi/4)$	$\nu \in$(15,30)[m/s]

When investigating the effects of particular parameters, such as ρ, R and c_0, their value was varied in the range ±10%.

•The real energy dispersion in the system ought to take into account the 'negative damping', associated with the phase shift of the function w and equal to

$$\beta = \omega_4\tau_0 \tag{13}$$

between the axial stresses in the band and the function w. This effect is illustrated in Fig. (4)

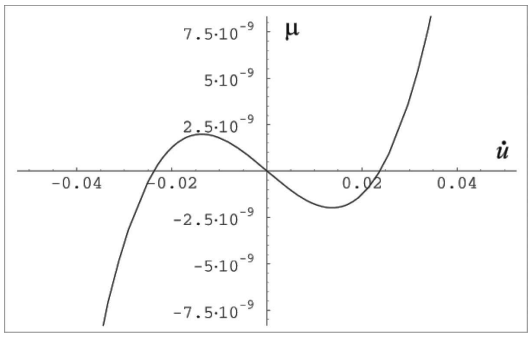

Fig. 4. Damping model taking into account the 'negative damping'. $\mu = \gamma_1\dot{u} + \gamma_2\dot{u}^3$(see eq. (11,12))

It appears that for middle values of the parameters listed below and for $\beta = \pi/5$ and ω_4 =4559[rad/s], vibrations occur in the roller-band system associated with the limit cycle defined by the zero of the characteristic. It is a typical effect, occurring in self-excited systems. The appearance and scale of this cycle depend chiefly on parameters in the calculation procedure, particularly β, ε_1 and ε_2.

•Numerical simulation data reveal that vibration amplitudes fall in the range (0-100)[μm] and vibrations appear to be nearly perfectly harmonic, which is corroborated by Fig. (5), showing the time patterns of the vibration and its spectral analysis.

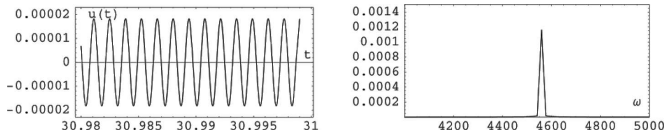

Fig. 5. Function u(t) and its FFT transform. Parameters taken in calculations: Δh_0 =2*10^{-4}[m], ν =25[m/s], $\beta = \pi/5$. The remaining parameters are summarised above

That fully confirms the adequacy of the applied approximation, where the delayed argument function w is replaced by the linear combination of a function and its derivative with respect to time.

•Among parameters used in this study, those involving the highest level of uncertainty include damping factors, ε_1 and ε_2. Generally speaking, the values quoted in major publications [6, 11] are of the order of 10^8. It seems fully merited to compare those parameters with the relevant values given in the literature on the theory of vibrations with reference to steel deformation processes [8]. This should not present any major difficulty since the differential equation describing the roll motion becomes an equation of an nonlinear, 1 DOF oscillator. To handle such equations, a dimensionless coefficient ζ is introduced associated with the linear component of damping related to the mass and elasticity of the oscillator.

$$\omega_{00}^2 = \frac{\dfrac{k\alpha c_1}{GA} + \dfrac{GAc_2}{kEJ} + c_4 - \dfrac{GAc_5}{kEJ} - c_6 - c_7}{\dfrac{k\rho c_1}{G} + \dfrac{\rho c_2}{E}} \qquad \frac{k\alpha\left(\dfrac{\varepsilon_1 \Delta h_0}{\sigma^*} + \dfrac{3}{8}\dfrac{\varepsilon_2 v^2 \Delta h_0^2}{\sigma^*}\right)}{GA\left(\dfrac{k\rho c_1}{G} + \dfrac{\rho c_2}{E}\right)} = 2\omega_{00}\zeta \tag{14}$$

In this case the middle values of the relevant coefficients are taken and v =23[m/s], $\beta = \pi/5$,ω_4 =4559[rad/s] (726[Hz]) and finally we obtain:.

$$\zeta = 0.03271 \tag{15}$$

This value is very near to that assumed in the theory of vibrations. It is reasonable to suppose, therefore, that the value of coefficient ε_1 is selected correctly. Parameters ε_2 and β in the simulations are controlled such that that for the predetermined variability range of the system's parameters, the amplitudes should fall in the interval (0-100)[μm].

•For parameters of the rolling process and the rolling machine fluctuating round their medium values, the amplitudes of vibration range from 0 to 100[μm]. Figures below show the effects of major parameters on maximal amplitudes, derived from the formula:

$$a = X_4(\frac{l}{2})u(t)_{max} \tag{16}$$

Amplitude variability characteristics are obtained at four velocity levels: 15, 20, 25, 30 [m/s]. Equivalent density ρ has no physical interpretation, nevertheless, it may be used in evaluating the total mass of the working and backing rolls. It is readily apparent that its increase leads to intensification of vibration. Fig. (6) shows the amplitude-draft Δh_0 relationship, which is decidedly stronger than that between the amplitude and roll mass. For small drafts, of the order of 0.1 [mm], the amplitudes attain high values, approaching 140 [μm] and for the medium draft they range from 20 to 50 [μm], depending on the actual rate of travel.

An increase of this velocity has the damping effect on the amplitude.

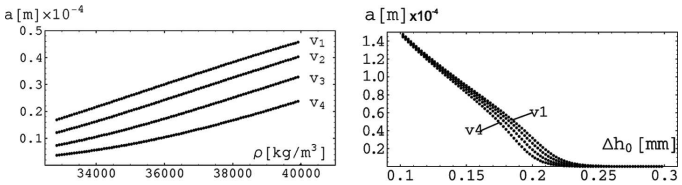

Fig. 6. The effects of the roll mass (A) and the draft (B) on vibration amplitudes for the rate of travel: v_1 =15,v_2 =20,v_3 =25,v_4 =30[m/s]

Fig. (7) shows how geometric and elastic properties of the rolling stand impact on the intensity of vibrations. One has to bear in mind, however, that only the curves obtained for v=25 and 30[m/s] are of some importance for the rolling processes. Such rates are characteristic of the final rolling stand in the rolling line. The remaining rolling rates can be implemented in the second or third stand from the end.

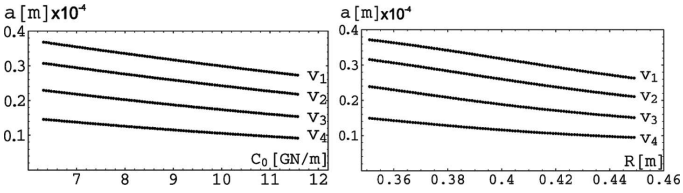

Fig. 7. The effects of the equivalent roll radius and rolling stand rigidity on vibrations amplitude at the band centre, for the rates of travel: v_1 =15,v_2 =20,v_3 =25,v_4 =30[m/s]

It is reasonable to suppose that the properties of the rolling stand have a minor bearing on vibration intensity, unlike the process parameters whose role seems predominant. It is illustrated in Fig. (8) showing the effects of the rate of travel on the amplitude of roll vibrations in the middle of the band.

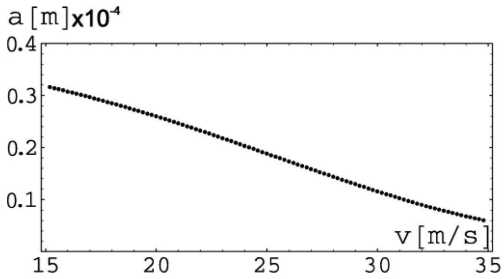

Fig. 8. Vibrations amplitude in the middle of the band vs the rate of travel v. The remaining parameters are assumed to have the middle values

The decay threshold is assumed at amplitudes less than 5 [μm], hence one is able to find the regions of vibration occurrence in the domain of two selected parameters. Such 'map' is shown in Fig. 9.

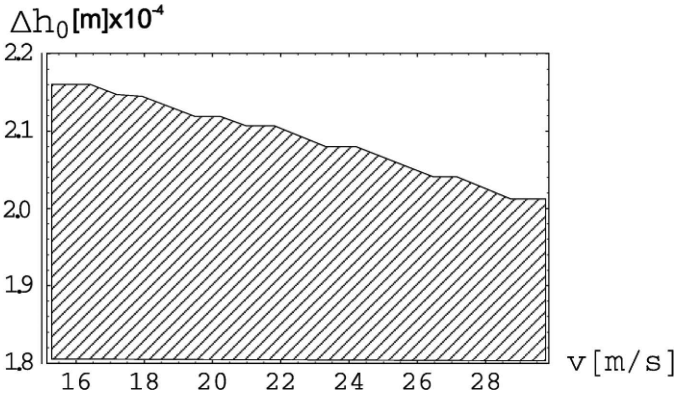

Fig. 9. Regions of vibration occurrence in the domain of travel rate and draft

Knowing the position function $X_4(x)$ and the function of time $u(t)$ yielding the vibration amplitudes at selected roll sections, we are now able to explain the appearance of darkened streaks on the surface of the sheet being rolled. The analysis of the problem is briefly summarised below. In accordance with the description of physical aspects of the rolling processes, the velocities when leaving the rollgap are different for various filaments of the sheet being rolled, depending on their actual distance from its centre of thickness. Most authors take this distribution pattern to be parabolic, which is shown in Fig. (10).

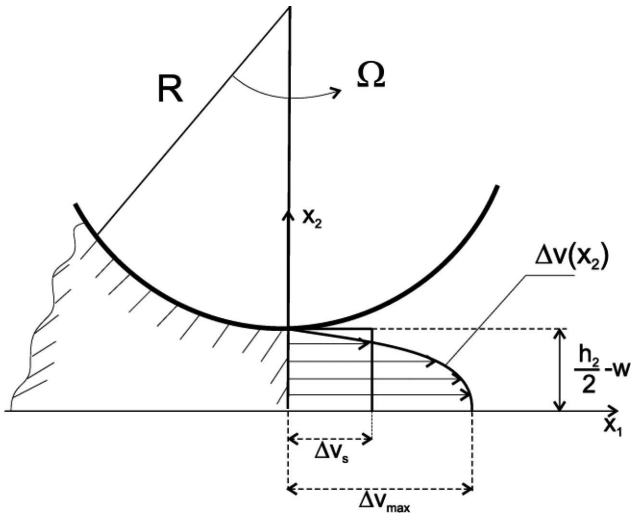

Fig. 10. Distribution of velocity increment Δ v in particular band filaments

Δv denotes the increment of velocity of a filament positioned inside the band with respect to the quantity ΩR, defining the velocity of filaments in contact with the roll, assuming no slipping. The quantity Δv_s stands for the average value of this increment derived from the equation of stream continuity, the spacing between the rolls being varied by $2w(x,t)$:

$$h_1 v_{10} = (h_2 - 2w)(v_{20} + \Delta v_s)$$

In steady state conditions $h_1 v_{10} = h_2 v_{20}$, we are able to obtain Δv_s:

$$\Delta v_s = 2v_{20}\frac{w(x,t)}{h_2 - 2w(x,t)} = 2v_{20}X_4(x)\frac{u(t)}{h_2 - 2X_4(x)u(t)} \quad (17)$$

v_{10} and v_{20} in the formulas above define the velocities at the rollgap inlet and outlet, in steady-state conditions (no vibrations). The positioning function $X_4(x)$ defines the fourth mode of roll vibrations (bending line) under high-frequency vibrations. In accordance with the assumption of parabolic distribution of the function Δv:

$$\Delta v \cong \frac{\Delta v_{max}}{h_2^2}(h_2^2 - 4x_2^2) \quad (18)$$

Hence:

$$\Delta v_s = \frac{2}{h_2}\int_0^{\frac{h_2}{2}} \Delta v dx_2 = \frac{2}{3}\Delta v_{max} \quad (19)$$

Extensions Δs of particular filaments follow a similar pattern. Accordingly, we get:

$$\Delta s \cong \frac{\Delta s_{max}}{h_2^2}(h_2^2 - 4x_2^2) \;\; ; \;\; \Delta s_s = \frac{2}{3}\Delta s_{max} \quad (20)$$

$$\Delta s_s = \int_0^{\frac{T}{2}} \Delta v_s dt \;\; ; \;\; T = \frac{2\pi}{\omega_4} \quad (21)$$

Function $\Delta s(x_2)$ yields the shear angle δ of external filaments, assuming no slipping. The angle is equal to:

$$\delta = \Delta s'(\frac{h_2}{2}) = -\frac{4\Delta s_{max}}{h_2} = -\frac{6\Delta s_s}{h_2} \quad (22)$$

Under these assumptions, the shearing stress in external filaments is given as:

$$\tau = G|\delta| = \frac{6G\Delta s_s}{h_2} \quad (23)$$

Assuming h_2 =0.4[mm], v =25[m/s], Δh_0 =0.18[mm] and for remaining parameters given in (13), the shearing stress is given as:

τ_1 =4.24*10^{12}[Pa] When Δh_0 is increased to 0.2[mm], this value is equal to:

τ_2 =1.1554*10^{11}[Pa] Both stress values vastly exceed the critical shear stress limit, which is equal to 160[MPa]. It appears that the 'no-slipping' assumption must not be maintained. Slipping occurring every period of the function u(t) damages the surface of the steel sheet being rolled, leading to formation of characteristic streaks. The spacing between those streaks is given by the simple formula:

$$\lambda = \Omega R\frac{2\pi}{\omega_4} \quad (24)$$

For parameters considered in this study and for v =25[m/s], this spacing becomes λ =0.034[m]. This value falls in the interval of spacing value registered in real rolling systems [7].

Results imply that the physical model of high-frequency vibrations proposed by the authors is correct and adequate.

7. Conclusions

The value of frequency and amplitudes of self-excited vibrations observed in a simulation of the mathematical model of four-high mill are along with those found in real objects.

This allows to conclude that the suggested model was appropriate and may be applied in analysis of the issue in question. It is especially important if we consider that it is the first time the reference literature presents this model as a key to clarify the appearance of strips on the surface of a rolled metal plate. In the case of four-high mills, the self-excited vibrations appear in the last rolling stands milling with small drafts.

Simulation results indicate that in order to reduce the consequences of such vibrations, the drafts may not exceed the value of Dh_0 = 0.22 mm

The second technological parameter having a substantial influence of the course of this process is the speed of rolling which if reduced, has an impact on the drop of vibrations amplitude. This observation allows to adjust far better monitoring and control over the process in question.

REFERENCES

[1] A. B a r, A. Ś w i ą t o n i o w s k i, Analysis of chattering phenomena in cold rolling structures Waves Biomedical Engeneering **10**, 1, (Structural Acoustic) 81-90 (2001).

[2] J. N i z i o ł, O. B a r, Drgania belki Timoshenki na nieliniowym podłożu z uwzględnieniem harmonicznego wymuszenia i rozpraszania energii, Czasopismo Techniczne 5-M, 243-255 (2004).

[3] A. Bar, O. Bar, Types of mid-frequency vibrations appearing during the rolling mill operation, Journal of Materials Processing Technology **162-163**, 15, 461-464 (2005).
[4] A. Bar, A. Świątoniowski, Parametrical excitements vibration in tandem mills-mathematical models and its analysis Journ. of Matterial Proc. Technology **134**, 214-224 (Elsevier) 215-225 (2003).
[5] A. Bar, A. Świątoniowski, Indepedence between the rolling speed and nonlinear vibration of the mill system Journ. of Matterial Proc. Technology **155-156C**, 2116-2121 (2004).
[6] Guo Remn-Min, A.C. Urso, Analysis of chatter vibration phenomena of rolling mills using finite element metods Iron and Steel Engineer, 29-39, January 1993.
[7] G.L. Nesler, J.F. Cory, Identifiction of chatter sources in cold rolling mills Iron and Steel Engineer, 40-45, January 1993.
[8] J. Niziół, Podstawy drgań w maszynach. Politechnika Krakowska, 1996.
[9] W.L. Roberts, Flat Processing of Steel New York and Basel, Marcel Decker Inc. 1987.
[10] A. Świątoniowski, A. Bar, Współczesne problemy wytwarzania blach i taśm Uczeln. Wydawn. Naukowo-Dydaktyczne AGH, Kraków 2005.
[11] J. Tlusty, G. Chandra, Chatter in Cold Rolling Annals of the CIRP **31**, 1, 195-199 (1982).
[12] J. Niziół, A. Bar, O. Bar, Samowzbudne drgania średnio i wysokoczęstotliwościowe występujące w procesie walcowania blach, WISNIK-Chmielnickij **1**, 213-222 (2003).
[13] A. Stefanik, P. Szota, H. Dyja, Numerical Modeling of the Microstructure During 50×20 mm Flat Bars Rolling Process, Archives of Metallurgy and Materials **54**, 3, 589-596 (2009).
[14] W. Hofmann, H. Aigner, Reduction of chatter marks during shin pass rolling of steel strips, Metallurgical Plant and Technology International **1**, 98-102 (1998).
[15] B. Hardwick, T.S. Dunlop, Application of vibration monitoring to cold mill processes. Iron and Steel engineer, 39-45 January 1999.
[16] Y.J. Lin, C.S. Suh, R. Langari, S.T. Noah, On the characteristics and mechanism of rolling instability and chatter. Journal of Manufacturing Science Eng. Trans. ASME **125**, 778-786 (2003).
[17] J. Mackel, Condition Monitoring and Diagnostic Engineering for Rolling Mills, Industrial Handbook, ACIDA, 2003.
[18] P. Montmitonnet, Hot and cold strip rolling processes. Comput. Methods Appl. Mech. Eng **195**, 6604-6625 (2006).
[19] S. Timoshenko, Strength of Materials, third ed. Krieger Publishing Co. 1983.
[20] Y.X. Wu, J.A. Duan, Frequency modulation of high speed mill chatter, Journal of Materials Processing Technology, 129 (2002).
[21] E. Brusa, L. Lemma, Numerical and experimental analysis of the dynamic effects in compact cluster mills for cold rolling, Journal of Materials Processing Technology, 2008.
[22] S. Wroński, K. Wierzbanowski, B. Bacroix, T. Chauveau, M. Wróbel, A. Rauch, F. Montheillet, M. Wroński, Texture heterogeneity of asymmetrically cold rolled low carbo steel, Archives of Metallurgy and Materials **54**, 1, 89-102 (2009).
[23] J. Zhong, H. Yan, J. Duan, L. Xu, W. Wang, P. Chen, Industrial experiments and findings on temper rolling chatter Journal of Materials Processing Technology **120** (1), 275-280, Jan 2002.
[24] S. Timoshenko, Vibration Problems in Engineering, Toronto New York London 1955.
[25] W. Nowacki, Dynamika budowli, Warszawa, Arkady 1972.

Received: 10 April 2012.